Supporting Information

Unprecedented binding mode of hydroxamate-based inhibitors of glutamate carboxypeptidase II: structural characterization and biological activity

Zora Novakova,[1] Krystyna Wozniak,[2] Andrej Jancarik,[6] Rana Rais,[2,3] Ying Wu,[2] Jiri Pavlicek,[1] Dana Ferraris,[7] Barbora Havlinova,[1] Jakub Ptacek,[1] Jan Vavra,[6] Niyada Hin,[2] Camilo Rojas,[2] Pavel Majer,[6] Barbara S. Slusher,[2,3,4,5]* Takashi Tsukamoto,[2,3]* and Cyril Barinka[1]*

Table of Contents of SI

Supporting Figure S1: Chiral separation of (*R*)-1 and (*S*)-1

(*R,S*)-1 was resolved into individual enantiomers by HPLC on a Eurocel 01 column (250 × 4.6 mm, 5 µm, Knauer) using an instrument consisting of an isocratic HPLC pump (Knauer Smartline 1000), a variable-wavelength UV detector set at 254 nm (Knauer Smartline 2500), a polarimetric detector (Chiralyser LED 426 nm, IBZ Messtechnik) and a PC workstation with Clarity software (Dataapex). n-Heptane-ethanol (2:1) was used as a mobile phase at a flow rate of 1.0 ml/min. For analyses, the samples were dissolved in HPLC ethanol (ca 1 mg/ml) and filtered through a 0.45 µm PTFE syringe filter before injection (ca 1 µl). Concentrations of samples for preparative separations were 10 mg/ml of the racemate for each run (injection 1 ml). Column for preparative separations was Eurocel 01 (270 x 25 mm, 5 µm, Knauer).

HPLC (Eurocel 01 column) of racemic hydroxamic acid (red: UV detector, blue: downstream polarimetric detector):

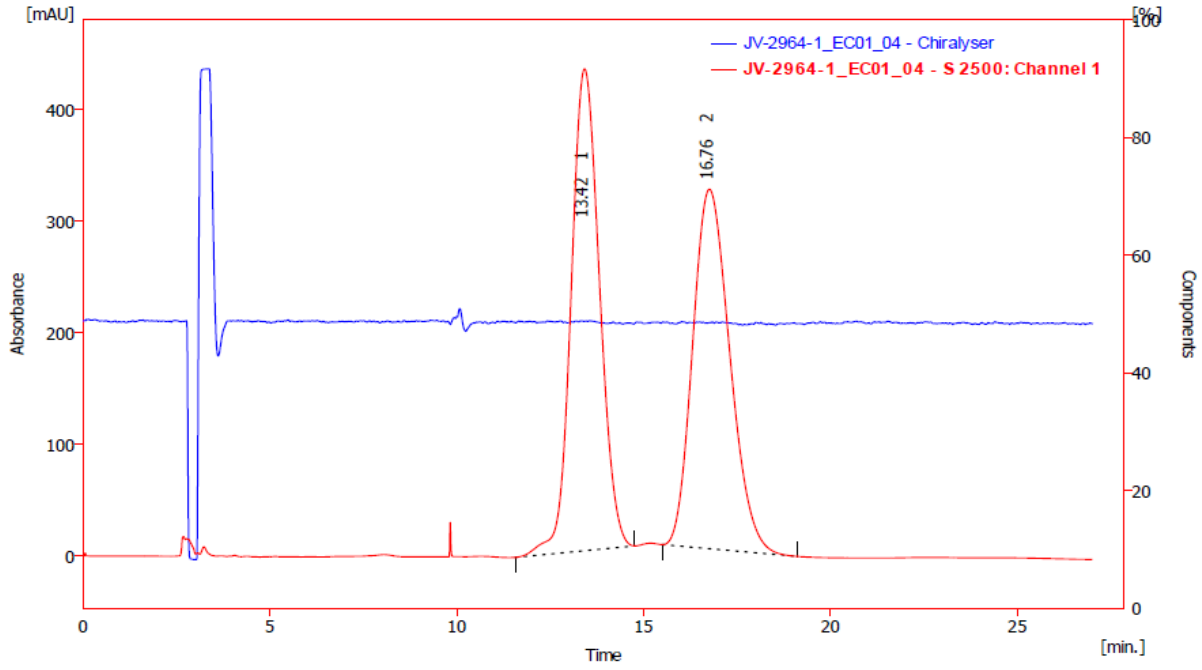

Result Table (Uncal - JV-2964-1_EC01_04 - S 2500: Channel 1)

	Reten. Time [min]	Area [mAU.s]	Height [mAU]	Area [%]	Height [%]	W05 [min]	Compound Name
1	13.423	22817.400	431.629	50.66	57.3	0.82	
2	16.763	22218.928	322.055	49.34	42.7	1.08	
	Total	45036.328	753.684	100.00	100.0		

HPLC (Eurocel 01 column) of pure enantiomers of tribenzyl esters **(*R,S*)-1** (red: UV detector) after chiral HPLC semipreparative resolution.

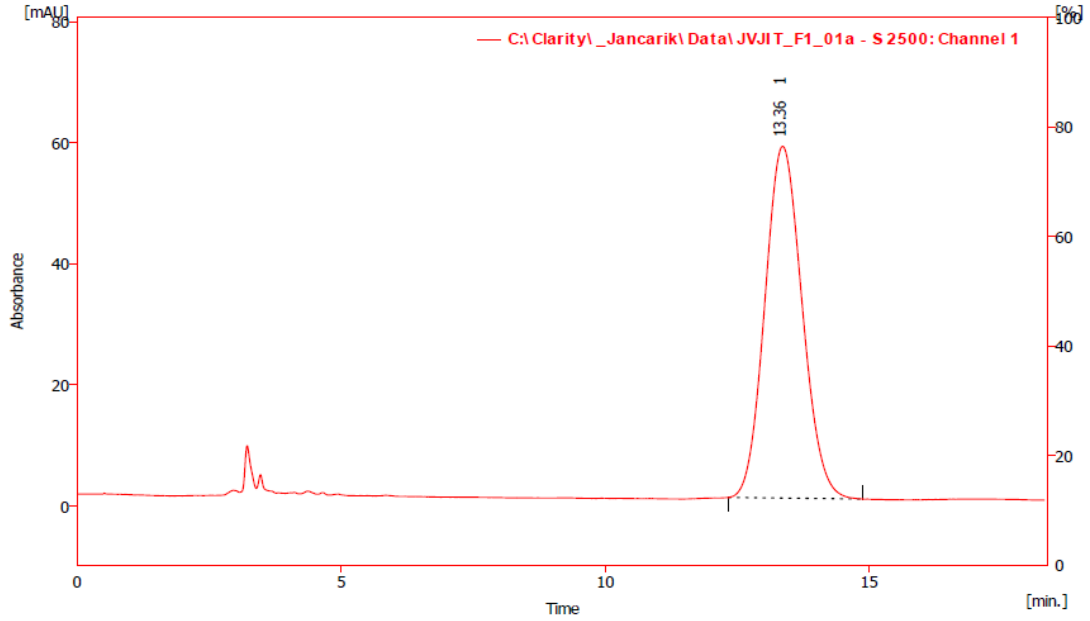

Result Table (Uncal - C:\|Clarity\|_Jancarik\|Data\|JVJIT_F1_01a - S 2500: Channel 1)
Drift (11.59-14.51 min.): 10.5028 [mAU/h]

	Reten. Time [min]	Area [mAU.s]	Height [mAU]	Area [%]	Height [%]	W05 [min]	Compound Name
1	13.357	2850.491	58.067	100.0	100.0	0.77	
	Total	2850.491	58.067	100.0	100.0		

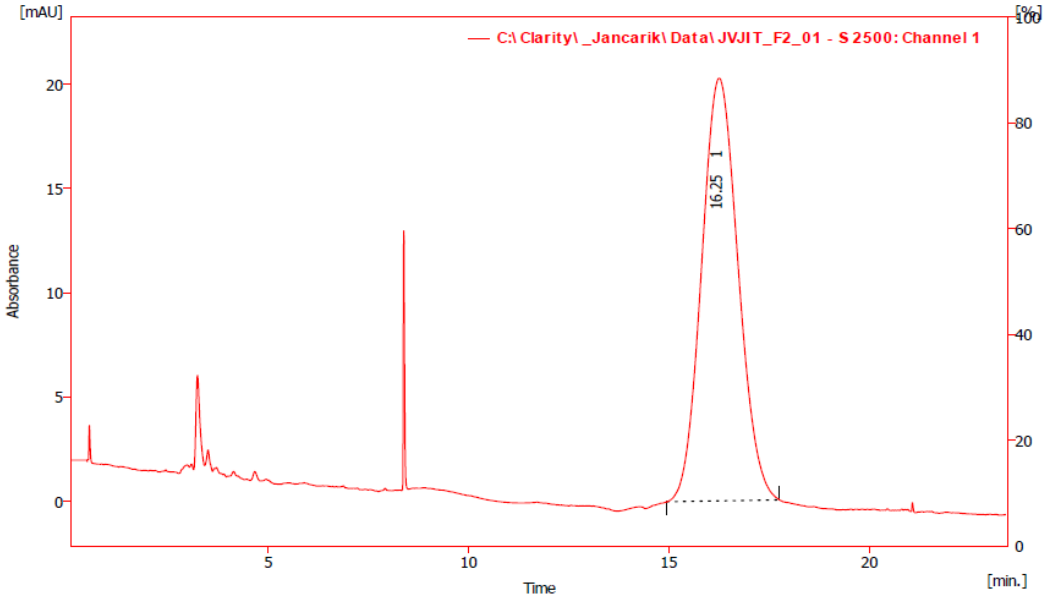

Result Table (Uncal - C:\|Clarity\|_Jancarik\|Data\|JVJIT_F2_01 - S 2500: Channel 1)

	Reten. Time [min]	Area [mAU.s]	Height [mAU]	Area [%]	Height [%]	W05 [min]	Compound Name
1	16.250	1285.239	20.268	100.0	100.0	0.99	
	Total	1285.239	20.268	100.0	100.0		

Supporting Figure S2: GCPII/inhibitor distances

The table shows intermolecular distances between *(S)*-1, *(R)*-1 and GCPII atoms within the 4 Å radius. Nomenclature of inhibitor atoms is shown in the accompanying formula.

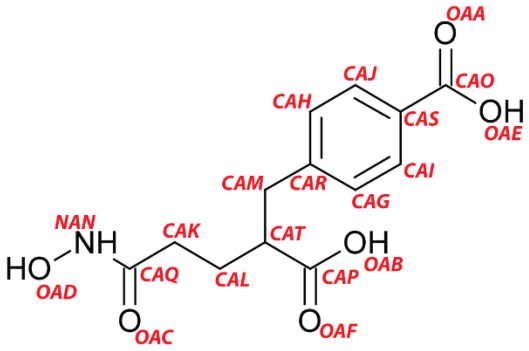

***(R)*-1**

inhibitor atom name	distance [Å]	protein atom name
OAE	2.5	Tyr234-OH
	3.6	Tyr234-CZ
	3.8	Tyr234-CE2
	3.9	Tyr552-CD2
	4.0	Tyr552-CE2
	3.2	HOH2111
OAA	3.5	Tyr234-OH
	3.8	Tyr234-CZ
	3.2	Tyr234-CE2
	3.5	Gly548-N
	3.2	Gly548-CA
	3.8	Gly548-C
	3.6	Tyr549-N
	3.6	Tyr552-CB
	3.4	Tyr552-CG
	3.0	Tyr552-CD2
	3.7	Tyr552-CE2
CAO	3.4	Tyr234-OH
	3.9	Tyr234-CE2
	3.6	Gly548-N
	3.6	Gly548-CA
	3.3	Tyr552-CD2
	3.5	Tyr234-CE2
CAS	3.9	Gly548-N
	3.6	Gly548-CA
	3.8	Tyr234-CZ
	3.5	Tyr234-CE2
	3.7	Tyr552-CD2
CAJ	3.8	Tyr552-CG
	3.7	Tyr552-CD2
	3.6	Tyr552-CE2
	3.6	Tyr234-CZ
	3.7	Tyr552-CE1
	3.8	Tyr552-CD1
	3.4	Gly548-CA
CAH	3.9	Tyr234-CZ
	3.9	Tyr552-CE1
CAM	3.6	Arg536-NH2
CAP	4.0	Arg536-NH2
	3.6	Arg534-NH1
	3.6	Arg534-NH2
	3.8	Asn519-ND2
OAB	3.9	Arg536-NH2
	3.0	Arg534-NH1
	3.8	Arg534-CZ
	3.7	Arg534-NH2
OAF	3.6	Arg534-NH1
	3.6	Arg534-CZ
	2.8	Arg534-NH2
	2.9	Asn519-ND2
	3.9	Asn519-CG
	2.8	HOH2434
CAL	3.6	Tyr552-OH
CAK	3.6	Tyr552-OH
	3.4	Gly518-O
	2.8	Act1-CH3
	3.6	Act1-C
	4.0	Act1-OXT
CAQ	3.9	Asp387-OD2
	3.3	Act1-CH3
	3.4	Act1-C
	3.4	Act1-OXT
OAC	3.3	Tyr552-CE1
	3.4	Tyr552-CZ
	2.7	Tyr552-OH
	3.9	Act1-O
	3.4	Act1-C
	3.4	Act1-OXT
	3.7	Act1-CH3
	3.7	Glu425-OE1
	3.2	Asp387-OD2
	3.0	His553-NE2
	3.3	His553-CE1
	2.1	Zn1751 (Zn1)
NAN	3.6	Asn519-ND2
	3.9	Glu425-OE1
	3.7	Act1-OXT
	3.4	Asp453-OD2
	2.8	Glu424-OE2
	3.4	Glu424-CD
	3.2	Glu424-OE1
	3.1	HOH2449
	3.0	Zn1751 (Zn1)
OAD	3.1	Glu424-OE2
	3.2	Glu424-CD
	2.7	Glu424-OE1
	3.9	His377-CD2
	3.0	His377-NE2
	3.7	His377-CE1
	3.2	Asp453-OD2
	3.3	Asp387-OD1
	3.7	Asp387-CG
	3.3	Asp387-OD2
	3.0	Glu425-OE2
	3.4	Glu425-CD
	3.3	Glu425-OE1
	2.8	HOH2449
	2.3	Zn1751 (Zn1)
	2.0	Zn1752 (Zn2)

***(S)*-1**

inhibitor atom name	distance [Å]	protein atom name
OAE	2.7	Tyr234-OH
	3.7	Tyr234-CZ
	3.9	Tyr234-CE2
	3.9	Tyr552-CD2
	3.0	HOH1828
OAA	3.3	Tyr234-CE2
	4.0	Tyr234-CZ
	3.6	Tyr234-OH
	3.4	Gly548-CA
	3.9	Gly548-C
	3.9	Gly548-N
	3.5	Tyr552-CG
	3.2	Tyr552-CD2
	4.0	Tyr552-CE2
	3.6	Tyr552-CB
	3.8	Tyr549-O
	3.5	Tyr549-N
CAO	3.3	Tyr552-CD2
	3.9	Tyr552-CG
	3.6	Tyr552-CE2
	3.8	Gly548-CA
	3.5	Tyr234-OH
	4.0	Tyr234-CE2
CAS	3.6	Tyr552-CD2
	3.5	Tyr552-CE2
	3.8	Tyr552-CZ
	4.0	Tyr552-CG
	3.8	Gly548-CA
CAJ	3.5	Tyr552-CG
	3.5	Tyr552-CD1
	3.6	Tyr552-CE1
	3.7	Tyr552-CD2
	3.8	Tyr552-CZ
	3.8	Tyr552-CE2
	3.6	Gly548-CA
CAH	3.9	Tyr552-CZ
	3.6	Tyr552-CE1
	3.8	Tyr552-CD1
CAL	3.9	Tyr700-OH
	3.7	Tyr700-CE1
CAI	3.9	Tyr552-CE2
	3.7	Tyr700-CE2
CAG	3.5	Tyr700-CE2
	3.9	Tyr700-CZ
	3.9	Tyr700-CD2
OAB	3.0	Arg534-NH2
	3.6	Arg534-NH1
	3.8	Arg534-CZ
	3.1	Asn519-ND2
	2.6	HOH1919
CAP	3.3	Asn519-ND2
	3.9	Arg536-NH1-B
	3.5	Arg534-NH2
	3.7	HOH1919
	3.5	HOH2072
OAF	3.2	Asn519-ND2
	3.4	Arg534-NH2
	3.2	Arg536-NH1-B
	2.8	HOH2072
	3.5	Asp453-OD2
	4.0	Asp453-CG
CAT	3.7	HOH2072
CAL	3.9	Tyr700-OH
	3.8	Tyr700-CZ
	3.7	Tyr700-CE1
	3.6	Tyr552-OH
	4.0	HOH1919
CAK	3.4	Act2140-O
	3.7	Act2140-CH3
	3.6	Act2140-C
	3.4	Gly518-O
	4.0	Tyr700-CE1
	3.8	Tyr552-OH
CAQ	3.4	Act2140-CH3
	3.6	Act2140-C
	3.9	Act2140-O
	3.5	Tyr552-OH
	3.9	Glu424-OE2
	2.9	Zn1751 (Zn1)
	3.8	Zn1752 (Zn2)
	3.2	HOH2072
	3.9	Asp387-OD2
OAC	2.7	Tyr552-OH
	3.4	Tyr552-CZ
	3.2	Tyr552-CE1
	3.3	His553-CE1
	2.9	His553-NE2
	3.2	Asp387-OD2
	2.1	Zn1751 (Zn1)
	3.5	HOH2072
	3.6	Glu425-OE1
	3.7	Act2140-CH3
	3.7	Act2140-C
	3.8	Act2140-O
NAN	2.8	Glu424-OE2
	3.4	Glu424-CD
	3.2	Glu424-OE1
	3.4	Asp453-OD2
	3.0	Zn1751 (Zn1)
	2.9	Zn1752 (Zn2)
	2.9	HOH2072
	3.7	Asn519-ND2
	3.9	Glu425-OE1
	3.9	Asp387-OD2
	3.6	Act2140-CH3
OAD	3.2	Glu424-OE2
	3.3	Glu424-CD
	2.8	Glu424-OE1
	3.0	His377-NE2
	3.6	His377-CE1
	3.9	His377-CD2
	3.3	Glu425-OE1
	3.4	Glu425-CD
	3.0	Glu425-OE2
	3.1	Asp387-OD2
	3.2	Asp387-OD1
	3.5	Asp387-CG
	2.2	Zn1751 (Zn1)
	1.9	Zn1752 (Zn2)
	3.2	Asp453-OD2
	2.6	HOH2072

Supporting Figure S3: Interaction pattern in the vicinity of active-site zincs.
Comparison of the zinc coordination sphere for hydroxamates (**panel a**), phosphorus-based (**panel b**) and urea-based (**panel c**) inhibitors. Coordination covalent bonds between the ZBGs and zinc ions (orange spheres) are shown as broken lines.

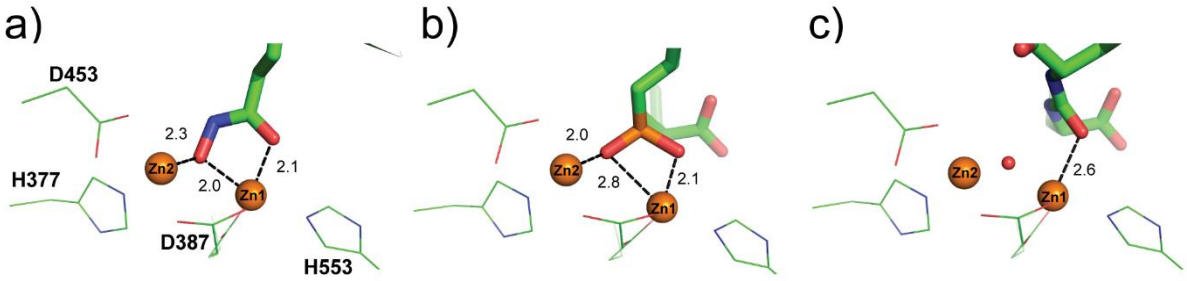

Supporting Figure S4: Superposition of *(R)*-1 and *(S)*-1 in the internal cavity of GCPII. Complexes of GCPII/***(R)*-1** and GCPII/***(S)*-1** were superimposed on corresponding Cα atoms of the enzyme and stereo representation is shown (**A**). Inhibitors are in stick representation and GCPII residues are shown as lines, with atoms colored red (oxygen), blue (nitrogen), and yellow and green (carbons) for ***(R)*-1** and **(*S*)-1**, respectively. The zinc ions are shown as orange spheres. Polar interactions between inhibitor and enzyme are shown for both enantiomers (dashed lines with colors corresponding to carbon atoms). Hydrogen-bound waters are shown by yellow and green spheres. Individual enantiomers are shown in panel **B** – ***(S)*-1** and **C** – ***(R)*-1.** Notice that stereochemistry at the chiral center has limited impact on the overall binding mode of studied hydroxamates and this finding is in line with virtually identical inhibition constants for both enantiomers.

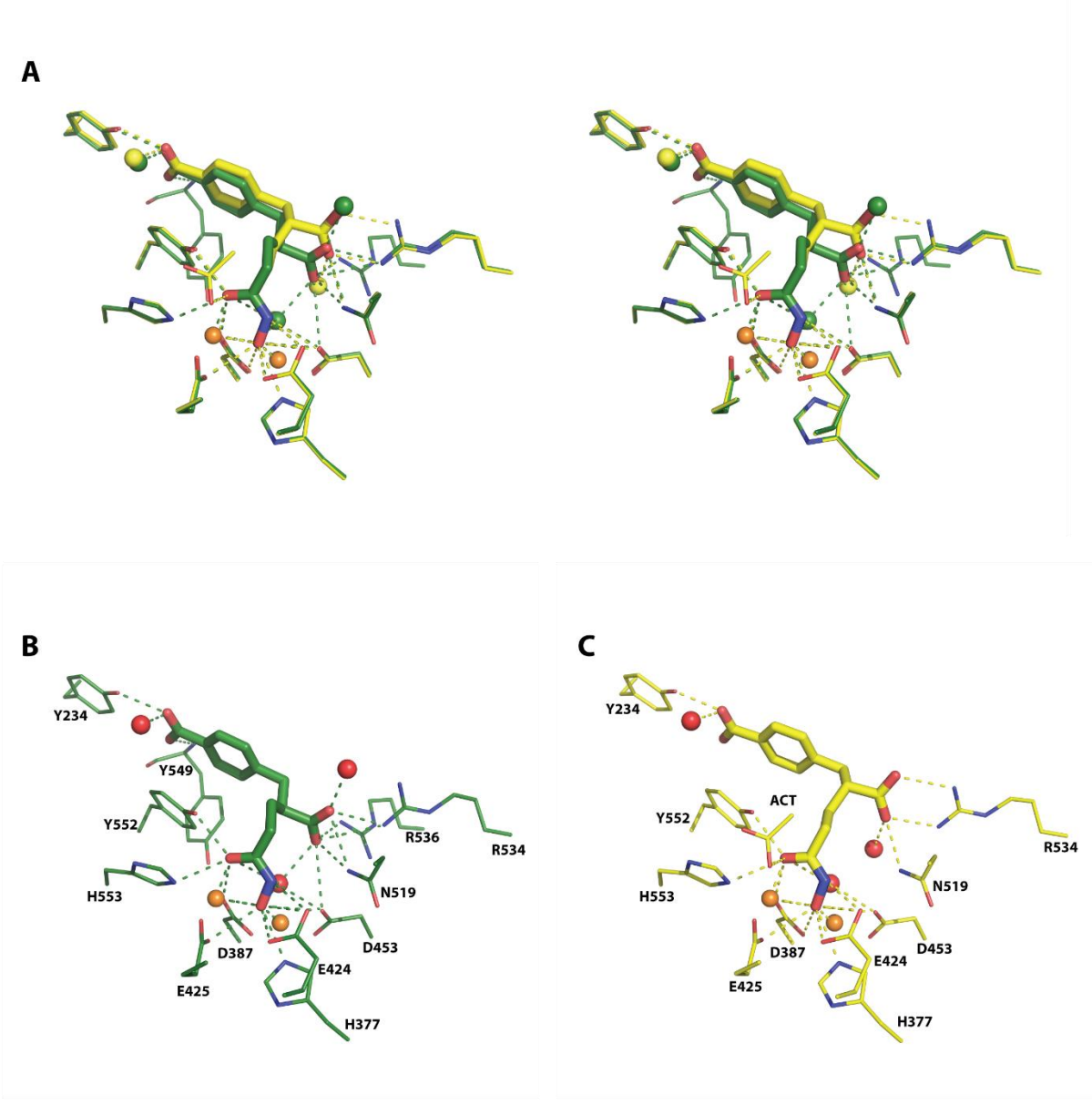

Supporting Figure S5: Inhibitory potency of hydroxamate-based compounds and *(R,S)*-19. Inhibition curves were determined using the fluorescence polarization method as described previously.[1] While ***(S)*-1**, ***(R)*-1** and ***(R,S)*-1** exhibit expected inhibition profile, none of remaining hydroxamate-based compounds (SAHA, TSA, acetohydroxamic acid) revealed any inhibition. These data indicate that the hydroxamate group alone is not sufficient for effective binding into the GCPII active site. Furthermore, the ***(R,S)*-19**, in which the hydroxamate ZBG is substituted by a carboxylate functionality with much weaker zinc-chelating properties, also failed to inhibit GCPII in the concentration range tested. The absence of GCPII inhibition by ***(R,S)*-19** implies that the synergy between the hydroxamate group and the S1 targeting moiety is indispensable for efficient inhibition.

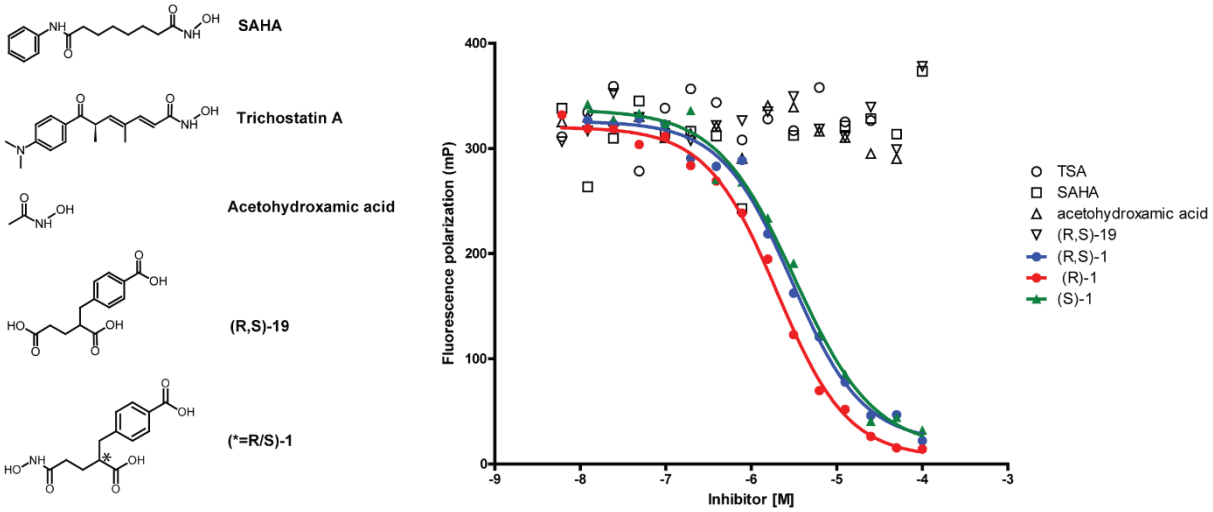

Supporting Figure S6: Inhibitory profiles of *(S)*-1, ***(R)*-1** and ***(R,S)*-1** for human GCP3**.** Inhibition curves determined by the radioenzymatic assay as described for GCPII (see main text for details). Corresponding IC_{50} values are 165 nM, 51 nM, and 70 nM for ***(R)*-1**, ***(S)*-1**, and ***(R,S)*-1**, respectively.

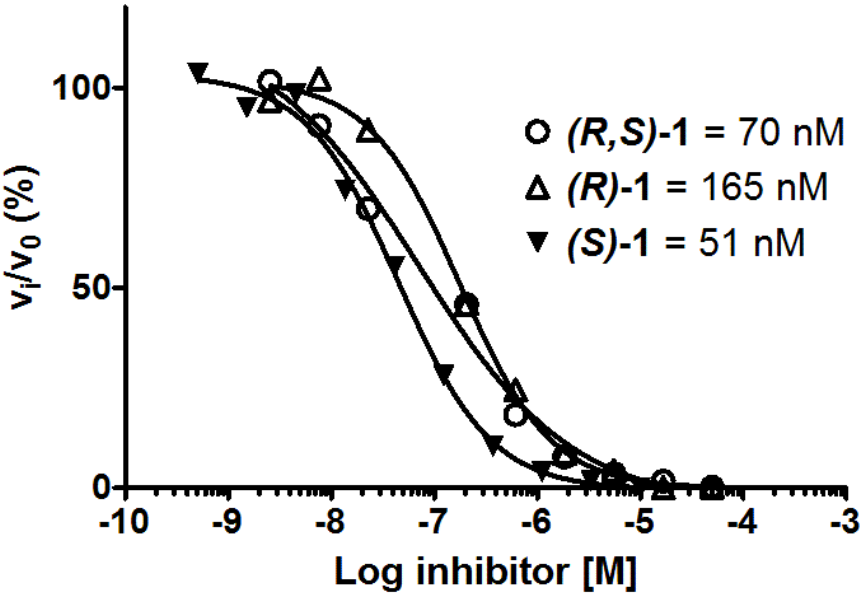

Supporting Figure S7: Superposition of GCPII and GCP3 highlighting residues of the S1 pocket interacting with (*S*)-1.

GCPII/***(S)*-1** complex and GCP3 (pdb code 3FEE) were superimposed on corresponding Cα atoms. ***(S)*-1** is shown in stick representation and GCPII residues interacting with the inhibitor are depicted in line representation (numbered according to GCPII). Atoms are colored by element – carbon is green and orange for GCPII and GCP3, respectively, oxygen is red, nitrogen is blue, zincs are shown as orange spheres and chlorine ion as magenta sphere. Notice the structural overlap between corresponding residues of GCPII/GCP3 implicated in interactions with ***(S)*-1**. This observation is in line with virtually identical inhibition constants of ***(S)*-1** for both paralogs.

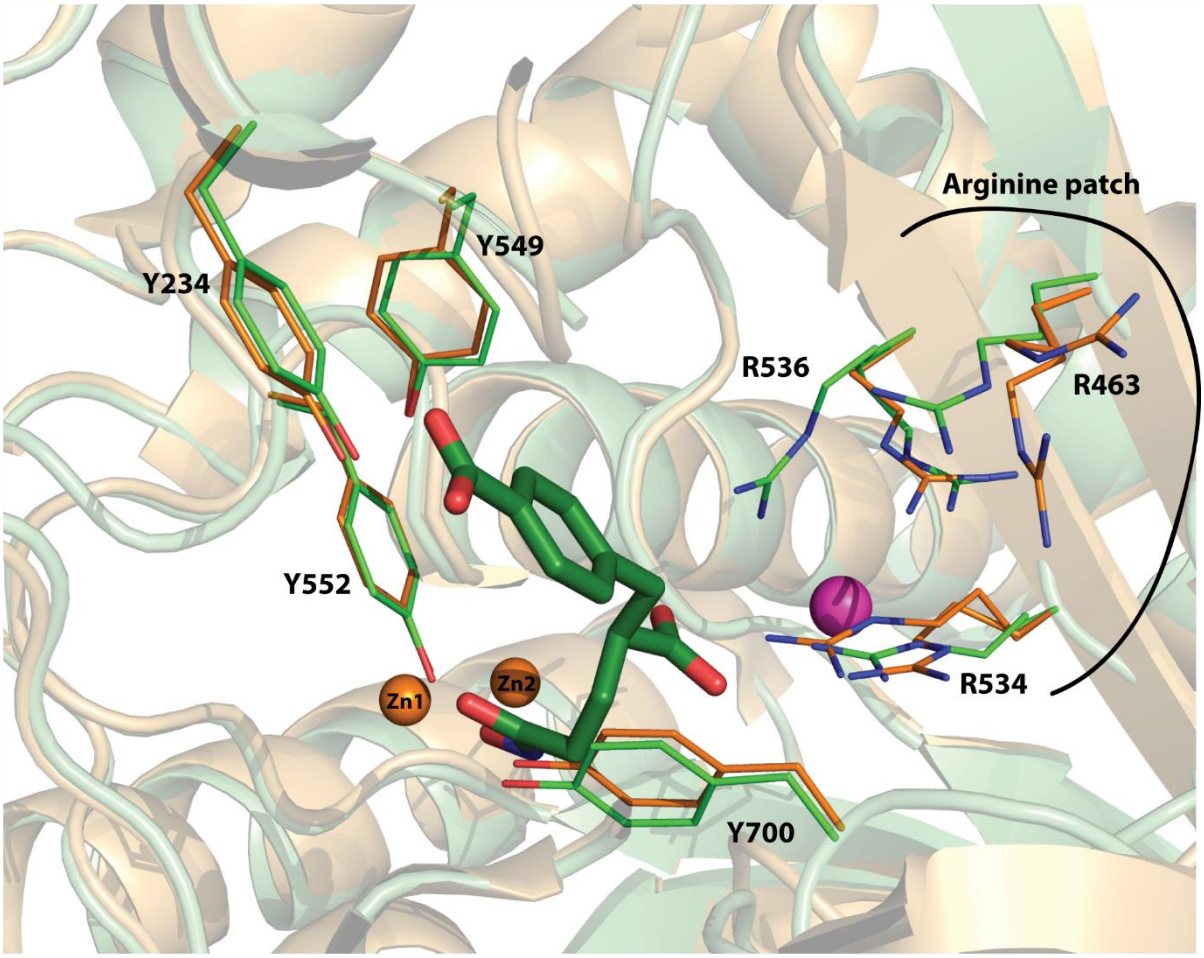

Supporting Figure S8: Sequence alignment of human GCPII and GCP3.

The alignment was done using Clustal W (1.83) software. Amino acid numbering is based on the GCPII sequence. Residues forming S1' and S1 pockets are marked with red and green dots, respectively.

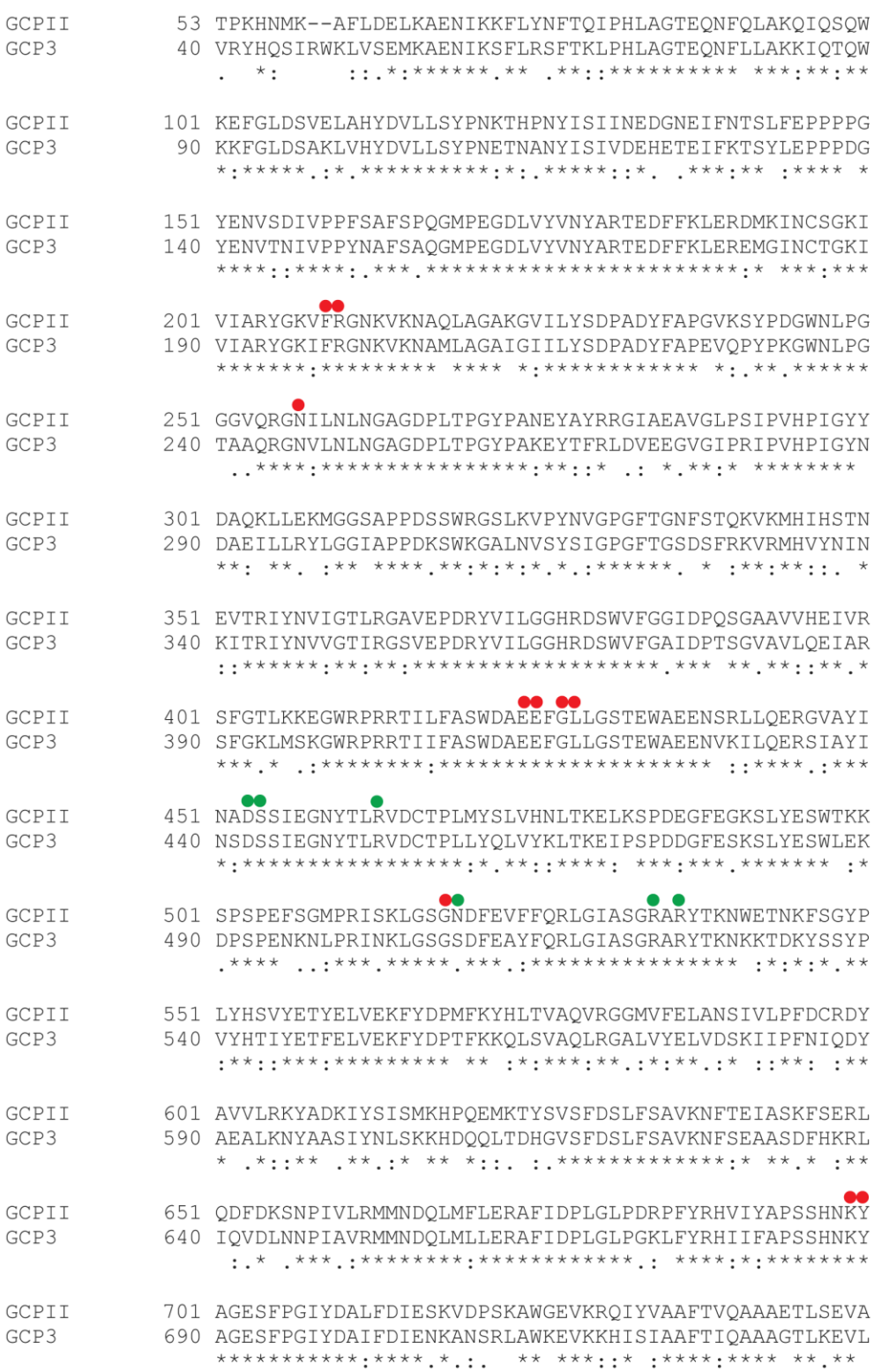

Supporting Materials and Methods

Supporting Scheme 1

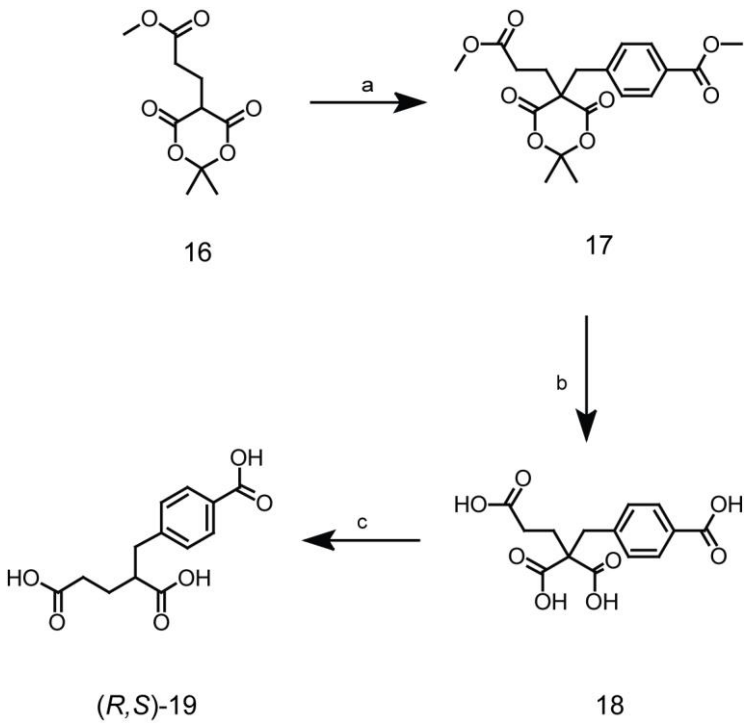

Methyl 4-((5-(3-methoxy-3-oxopropyl)-2,2-dimethyl-4,6-dioxo-1,3-dioxan-5-yl)methyl)benzoate; 17

To a solution of methyl 3-(2,2-dimethyl-4,6-dioxo-1,3-dioxan-5-yl)propanoate (226 mg, 1.0 mmol) in acetonitrile (3ml) benzyltriethylammoniumchlorid (228 mg, 1.0 mmol), methyl-4-bromomethylbenzoate (275mg, 1.2 mmol) and potassium carbonate (138 mg, 1.0 mmol) were added respectively and the mixture was stirred at room temperature under the nitrogen atmosphere for 2 h. Volatiles were removed *in vacuo*, the residue was dissolved in ethyl acetate (25 ml), and washed with 10% aq. $KHSO_4$ (2x), sat. $NAHCO_3$ (2x) and brine (1x), the organic layer was dried over anhydrous $MgSO_4$. Solvent was removed *in vacuo* and the residue was chromatographed on silica gel (hexane – ethyl acetate 3:1) to afford 189 mg (50 %) as a white amorphous solid.

^{1}H NMR (400 MHz, $CDCl_3$): 0.71 (3H, s), 1.60 (3H, s), 2.38 – 2.41 (2H, m), 2.48 – 2.51 (2H, m), 3.38 (3H, s), 3.68 (3H, s), 3.89 (3H, s), 7.25 – 7.27 (2H, m), 7.93 – 7.95 (2H, m).

^{13}C NMR (101 MHz, $CDCl_3$): 29.24, 29.33, 29.83, 35.41, 43.25, 52.18, 52.37, 56.09, 106.28, 129.82, 130.18, 130.67, 140.17, 166.17, 168.26 (2C), 171.69.

ESI MS: 401 ($[M + Na]^+$).

HR ESI MS: calcd for $C_{19}H_{22}O_8Na$ 401.12069; found 401.12074.

4-(4-carboxyphenyl)butane-1,3,3-tricarboxylic acid; 18

To a solution of methyl 4-((5-(3-methoxy-3-oxopropyl)-2,2-dimethyl-4,6-dioxo-1,3-dioxan-5-yl)methyl)benzoate (188mg, 0.5 mmol) in dioxane (3ml) was added NaOH (200 mg dissolved in minimal amount of water). The mixture was heated to 50°C for 5 h. After this period dioxane was evaporated and pH was acidified by 10% aq. $KHSO_4$. The aqueous phase was extracted with ethyl acetate (3 x 8 ml). Combined organic portions were dried over anhydrous $MgSO_4$, evaporated and the product was used in the next step without further purification.

2-(4-carboxybenzyl)pentanedioic acid; (*R,S*)-19

The solution of 4-(4-carboxyphenyl)butane-1,3,3-tricarboxylic acid (155 mg, 0.5 mmol) in DMSO (2 ml) was heated to 130°C for 5 h. The volatiles were removed *in vacuo* and the final product was purified on reverse phase column YMC (C18, 250x20mm) using a preparative HPLC system (pumps PU-986 (Jasco), UV detector UV-975 (Jasco) set at 230 nm, PC workstation with Clarity software (Dataapex)). Gradient 15-50% ACN in 60 min. with flow rate 10 ml/min.

^{1}H NMR (400 MHz, DMSO): 1.63 – 1.76 (2H, m), 2.17 – 2.31 (2H, m), 2.59 – 2.66 (1H, m), 2.77 – 2.82 (1H, m), 2.86 – 2.92 (1H, m), 7.31 (2H, d, *J* = 8.3), 7.85 (2H, d, *J* = 8.3), 12.41 (3H, s).

^{13}C NMR (101 MHz, DMSO): 26.71, 31.38, 37.37, 45.61, 128.79, 129.04, 129.31, 144.71, 167.24, 173.86, 175.64.

ESI MS: 265 ($[M - H]^-$).

HR ESI MS: calcd for $C_{13}H_{13}O_6$ 265.07176; found 265.07126.

REFERENCES

1. Alquicer, G.; Sedlak, D.; Byun, Y.; Pavlicek, J.; Stathis, M.; Rojas, C.; Slusher, B.; Pomper, M. G.; Bartunek, P.; Barinka, C. Development of a high-throughput fluorescence polarization assay to identify novel ligands of glutamate carboxypeptidase II. *J Biomol Screen* **2012,** 17, 1030-1040.